Biochemical and Biophysical Research Communications 460 (2015) 267–273

Contents lists available at ScienceDirect

Biochemical and Biophysical Research Communications

journal homepage: www.elsevier.com/locate/ybbrc

Graphene substrate for inducing neurite outgrowth

Jeong Soon Lee [a, 1], Alexey Lipatov [b, 1], Ligyeom Ha [a], Mikhail Shekhirev [b], Mohammad Nahid Andalib [a], Alexander Sinitskii [b, c, **], Jung Yul Lim [a, d, *]

[a] Department of Mechanical and Materials Engineering, University of Nebraska-Lincoln, Lincoln, NE 68588, USA
[b] Department of Chemistry, University of Nebraska-Lincoln, Lincoln, NE 68588, USA
[c] Nebraska Center for Materials and Nanoscience, University of Nebraska-Lincoln, Lincoln, NE 68588, USA
[d] The Graduate School of Dentistry, Kyung Hee University, Seoul, South Korea

ARTICLE INFO

Article history:
Received 27 February 2015
Available online 13 March 2015

Keywords:
Graphene
Retinoic acid
Neurite outgrowth
Neuronal gene expression
Neural regenerative medicine

ABSTRACT

A few recent studies demonstrated that graphene may have cytocompatibility with several cell types. However, when assessing cell behavior on graphene, there has been no precise control over the quality of graphene, number of graphene layers, and substrate surface coverage by graphene. In this study, using well-controlled monolayer graphene film substrates we tested the cytocompatibility of graphene for human neuroblastoma (SH-SY5Y) cell culture. A large-scale monolayer graphene film grown on Cu foils by chemical vapor deposition (CVD) could be successfully transferred onto glass substrates by wet transfer technique. We observed that graphene substrate could induce enhanced neurite outgrowth, both in neurite length and number, compared with control glass substrate. Interestingly, the positive stimulatory effect by graphene was achieved even in the absence of soluble neurogenic factor, retinoic acid (RA). Key genes relevant to cell neurogenesis, e.g., neurofilament light chain (NFL), were also upregulated on graphene. Inhibitor studies suggested that the graphene stimulation of cellular neurogenesis may be achieved through focal adhesion kinase (FAK) and p38 mitogen-activated protein kinase (MAPK) cascades. Our data indicate that graphene may be exploited as a platform for neural regenerative medicine, and the suggested molecular mechanism may provide an insight into the graphene control of neural cells.

1. Introduction

Graphene, a planar structure of carbon atoms arranged in a hexagonal lattice, receives a great deal of attention due to its unique electronic, mechanical, thermal, and optical properties and numerous potential applications in electronics, composites, energy storage, and other areas [1]. Several recent studies also proposed the potential of graphene and its derivatives, such as functionalized graphene and graphene oxide, for biomedical applications [2]. These include drug delivery, disease diagnostics, bioimaging, photothermal therapy, and antibacterial substrates [3–7]. With respect to the use of graphene for regenerative medicine, as a first step, a few studies have examined its cellular biocompatibility. Mesenchymal stem cells (MSCs) cultured on graphene did not show cytotoxicity effects and could accomplish osteogenic differentiation [8,9]. Neural stem cells and hippocampal cells cultured on graphene also showed cytocompatibility and enhanced neuronal differentiation [10,11]. When pristine graphene was modified with NH_2-group, it became more hydrophilic and supported the proliferation of mouse fibroblastic and human endothelial cells [12]. In assessing cell behavior on graphene, however, there has been no precise control over the quality of graphene, number of graphene layers, and substrate surface coverage by graphene. For instance, in some of these works on neural cell biocompatibility the base substrate (tissue culture polystyrene, TCPS) was not entirely covered with graphene [10,11]. See more discussion in Section 4 on the substrate integrity.

In this paper, we report the cellular neurogenesis on graphene-covered glass substrate with pristine glass coverslip used as a control. Graphene films were characterized by a number of microscopic and spectroscopic techniques and were proved to be

* Corresponding author. W317.3 Nebraska Hall, Lincoln, NE 68588-0526, USA. Fax: +1 402 472 1465.
** Corresponding author. 604C Hamilton Hall, Lincoln, NE 68588-0526, USA. Fax: +1 402 472 9402.
E-mail addresses: sinitskii@unl.edu (A. Sinitskii), jlim4@unl.edu (J.Y. Lim).
[1] These authors contributed equally.

http://dx.doi.org/10.1016/j.bbrc.2015.03.023
0006-291X/

monolayer and to fully cover the square glass substrate. We evaluated neurite outgrowth and key neural transcription factors on graphene and glass, and observed that graphene culture could induce cellular neurogenesis even without the help from the soluble neurogenic factor, retinoic acid (RA). Via inhibitor studies, a possible molecular mechanism of the graphene induction of cellular neurogenesis could also be proposed.

2. Materials and methods

2.1. Graphene growth and transfer onto glass substrate and characterization

Graphene films can be grown by the chemical vapor deposition (CVD) [13]. Using a home-built CVD system, the growth of graphene was performed on 25-μm-thick copper (Cu) foils (Alfa Aesar) as reported in our recent publication [14]. Briefly, the Cu foil was cleaned in acetic acid for 10 min, washed with water and isopropanol, and dried using nitrogen gas. The foils were then put into the CVD system and annealed in H_2 at 1000 °C for 30 min. Then, methane was introduced to the growth chamber and the graphene growth was performed at 1000 °C for 15 min in a CH_4:H_2 (1:1) atmosphere at a pressure of 420 mTorr. The Cu foil was removed from the heating zone and quickly cooled down to room temperature under the same CH_4:H_2 (1:1) atmosphere. Graphene films were then transferred onto glass microscope slides (15 × 15 mm^2) using a wet transfer method. For this, 4% polymethyl methacrylate (PMMA, M_w = 950,000) solution in anisole was spin-coated on one side of a graphene-covered Cu foil and dried. The unprotected graphene on the other side of the Cu foil was etched away by O_2 reactive ion etching (RIE, Trion Minilock Phantom III). Then, the foil was placed on the surface of a warm (50 °C) 1 M $Fe(NO_3)_3$ aqueous solution to etch away Cu. The remaining PMMA/graphene transparent film was washed in deionized water twice to remove $Fe(NO_3)_3$ residue. A clean glass slide was brought into contact with the transparent film and pulled from the water surface. The substrate was dried and washed twice in hot (50 °C) acetone to remove PMMA, leaving the graphene monolayer attached to the glass slide.

The structural quality of graphene was confirmed by Raman and UV–vis–NIR spectra. Raman spectra were recorded at ambient conditions using a DXR Raman microscope using a 532 nm laser at the power of 10 mW and a 100 × objective. UV–vis–NIR spectroscopy was performed using a Shimadzu UV-2401PC instrument in transmittance mode. Surface texture of graphene and control glass substrates was observed by atomic force microscopy (AFM) in the tapping mode using a Digital Instruments Nanoscope IIIa Dimension 3100. The root mean square surface roughness (R_q) was calculated using the AFM software. Water contact angle was measured by using a contact angle goniometer (Ramé-Hart 100-00). A water droplet of 10 μl was dropped and imaged, from which contact angle was measured.

2.2. Cell culture and neuronal differentiation

Human neuroblastoma SH-SY5Y cells (ATCC, CRL-2266) were maintained in Dulbecco's modified Eagle's medium supplemented with 10% fetal bovine serum and 1% penicillin-streptomycin (all from Invitrogen). Cells were seeded on glass coverslips (control) and glass coverslips coated with graphene, and placed in 12-well plates. Neurite outgrowth was induced by the treatment of cells with RA at 10 μM for 7 days with media changed every second day. For inhibitor studies, cells were treated with Y27632 (RhoA kinase or ROCK inhibitor, Selleckbio, 10 μM), FAK-14 (focal adhesion kinase or FAK inhibitor, Santa Cruz, 10 nM), PD98059 (extracellular signal-regulated kinase or ERK inhibitor, Santa Cruz, 10 μM), or SB203580 (p38 mitogen-activated protein kinase or p38 MAPK inhibitor, Santa Cruz, 10 μM) while inducing neural differentiation under RA. Cell viability and inhibition at these concentrations were confirmed beforehand (not shown).

2.3. Neurite length and number measurements

From optical cell images neurite length was measured by NeuronJ (ImageJ add-on). Methods followed our published protocol [15]. Briefly, using the NeuronJ the path of the neurite (straight or curved) was traced. The cellular extension was determined as a neurite from where a cell process had a width less than 3.85 μm (following our study [15]). For counting neurite number developed per cell, total number of neurites in the image were counted and the number was divided by the total number of cells in the image. Three repeated assays were performed and at least three images from each culture were taken. At least 50 neurites per condition were assessed for length measurement, and at least 100 cells per condition were used for counting the neurite number.

2.4. Immunofluorescence and RT-PCR

Microtubule-associated protein 2 (MAP2), a key neuronal marker, was observed by immunofluorescence. On day 7, cells were washed with phosphate buffered saline, fixed with 4% paraformaldehyde, permeabilized with 0.1% Triton X-100, and incubated in 1% bovine serum albumin solution. In detecting MAP2, chicken primary antibody specific to MAP2 (Abcam, ab5392) was used at 1:10,000 and fluorescein isothiocyanate (FITC)-tagged anti-chicken secondary antibody (Abcam, ab6749) at 1:1000. A Leica fluorescent microscope (DMI 4000B) was used to visualize MAP2.

Gene expression specific to neuronal markers was assessed by RT-PCR using our published protocol [16]. PCR primer pairs were as below. Neurofilament light chain (NFL): sense ACC TCC TCA ACG TGA AGA TGG CTT, anti-sense ACT CTT CCT TGG CAGC TTC TTC CT; Nestin: sense GCC CTG ACC ACT CCA GTT TA, anti-sense GGA GTC CTG GAT TTC CTT CC; MAP2: sense GCA TAT GCG CTG ATT CTT CA, anti-sense CTT TCC GTT CAT CTG CCA TT; GAPDH: sense CAT GAC CAC AGT CCA TGC CAT CAC T, antisense TGA GGT CCA CCA CCC TGT TGC TGT A. Three repeated culture assays were performed to obtain the data in Fig. 3C (n = 3).

2.5. Statistics

Means and standard deviations are presented in the figures. Statistical significance tested by one-way analysis of variance (ANOVA) followed by Student-Newman-Keuls tests is shown (see the legends in the figures).

3. Results

3.1. Monolayer graphene film could be successfully formed on glass substrate

Fig. 1A demonstrates optical images of a glass slide covered by graphene in comparison with a bare glass. Graphene film could be successfully coated on the square glass coverslip using our CVD-wet transfer method with no empty spot. The Raman spectrum of graphene formed on glass slide (Fig. 1B) showed sharp G and 2D bands at 1587 and 2680 cm^{-1}, respectively. Further, the D band was not observed around 1340 cm^{-1}, indicating that high quality graphene film was formed. The shape and position of the 2D band as well as the G-to-2D intensity ratio (about 1:2.5) are all characteristics of a monolayer graphene [17]. The transmittance of graphene was measured by UV–vis–NIR spectrometer with a blank glass

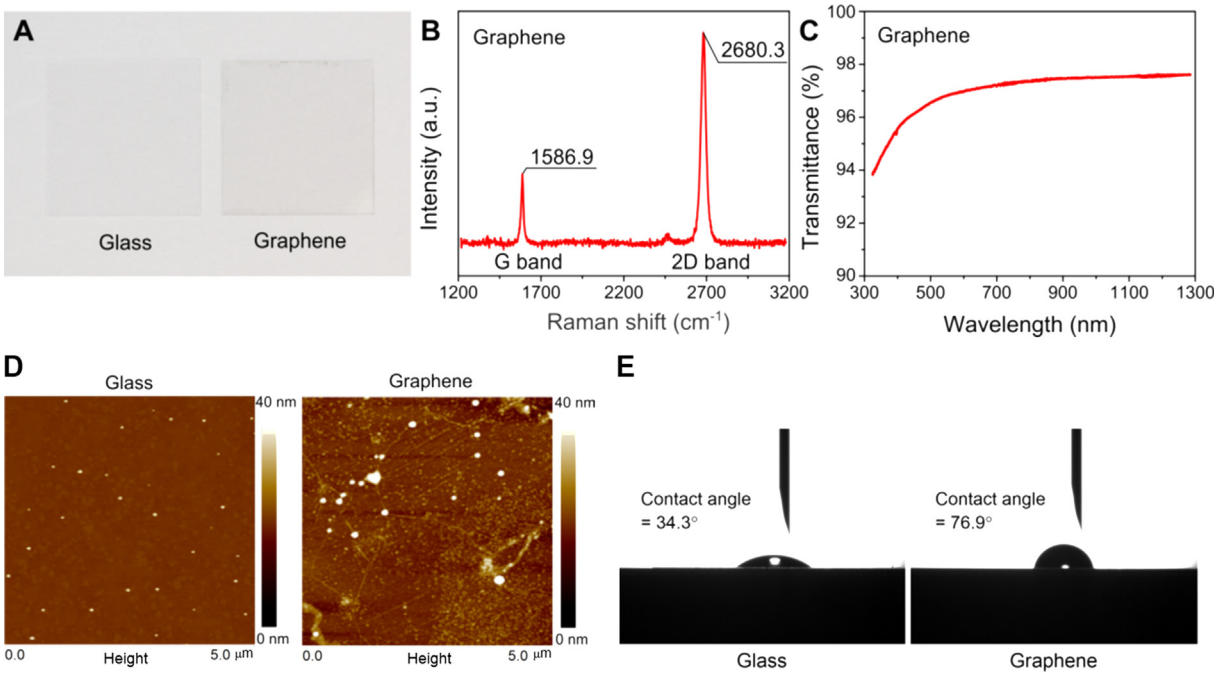

Fig. 1. Graphene monolayer film could be formed on glass slide for cell culture. (A) Optical images of a square glass slide (left) and glass slide covered with graphene film via CVD and wet transfer method (right). (B) Raman spectrum of graphene showed G and 2D bands. The 2D band shape and position and the G-to-2D intensity ratio (about 1:2.5) indicate the formation of a single-layer graphene. (C) UV–vis–NIR spectrum of graphene had 97–98% transmittance at 500–1300 nm, indicating that the graphene is monolayer. (D) AFM images of glass and graphene substrates. (E) Images of water contact with test surfaces by the sessile drop method and measured water contact angles.

slide used as a reference (Fig. 1C). The measured transmittance of 97–98% in the 500–1300 nm range provides additional evidence that the graphene film is monolayer [18]. Combined data indicates that a graphene single layered film could be successfully fabricated to fully cover the square glass coverslip. In AFM images (Fig. 1D), both surfaces were mostly flat and did not show any predetermined textures other than some occasional foreign particles and wrinkles. Roughness parameter (R_q), a root mean square deviation from the mean height line calculated by AFM, was very small for both surfaces (0.74 nm and 3.9 nm for glass and graphene, respectively). Water contact angle was 34.3° for glass and 76.9° for graphene (Fig. 1E), indicating that graphene is more hydrophobic than glass.

3.2. Neurite outgrowth is stimulated by graphene culture

To investigate the effect of graphene on neuronal differentiation of SH-SY5Y cells, we first tested neurite outgrowth, an apparent characteristic of neuronal differentiation that includes the development of axons and dendrites, under 10 μM RA treatment (a known soluble factor condition to induce the neurogenesis of SH-SY5Y cells [15,16]). Cells were imaged on day 7 (Fig. 2). RA induced neurite outgrowth on both control glass and graphene substrate as short as 7 days of exposure. Noticeably, cells cultured on graphene showed greater neurite development compared with cells on glass control. Neuronal differentiation was further confirmed by the immunofluorescence of MAP2 (Fig. 2 bottom), a primary neurogenesis marker. MAP2 was detected throughout the cell body and neurite process on both glass and graphene.

3.3. Neurite length and number and neural gene expression are enhanced on graphene

Neurite outgrowth was quantified as neurite length and number per cell. Experiments were repeated with or without RA treatment to reveal the exclusive and synergistic effect of graphene and RA (Fig. 3A). RA treatment on glass surface induced greater neurite length and number per cell relative to glass no RA control (Fig. 3B). Interestingly, graphene culture alone even in the absence of RA induced longer and more neurites compared with glass no RA control (*, **: $p < 0.05$ and 0.01, respectively, Fig. 3B). The number of neurite outburst per cell was not statistically different between the graphene no RA case and the glass but with RA case. RA and graphene provided synergistic effects to result in the greatest neurite length and number among the conditions tested.

To further test the neuronal differentiation on graphene, several neural mRNA expressions were assessed. Under RA, all neurotypical (NFL, nestin, and MAP2) mRNA expressions by SH-SY5Y cells were increased on two test surfaces (Fig. 3C). Interestingly, the expression of NFL, a key protein that composes the most abundant intermediate filament in neurons and axons [19], was significantly increased for cells on graphene even without RA treatment when compared with glass no RA control. Nestin (another intermediate filament in neuronal cells) and MAP2 gene expressions could also be detected on graphene even under no RA cue, though not as strong as NFL.

3.4. Graphene stimulation of neurogenesis may be achieved through FAK and p38 MAPK

To test the molecular mechanism of the graphene stimulation of cellular neurogenesis, we repeated experiments with RA but under inhibitors of several important molecular sensors. It was reported that downregulating ROCK by Y27632 has a potential to induce neurogenesis [20]. A similar phenomenon was observed on graphene culture such that longer neurites were obtained under Y27632 (Fig. 4; cell images in Supplementary Fig. S1). Notably, FAK-14 (FAK inhibitor) and SB203580 (p38 MAPK inhibitor) treatments significantly reduced both neurite length and number developed per cell (**: $p < 0.01$ compared with graphene no inhibitor control). Thus, the triggering of cellular neurogenesis by graphene may be

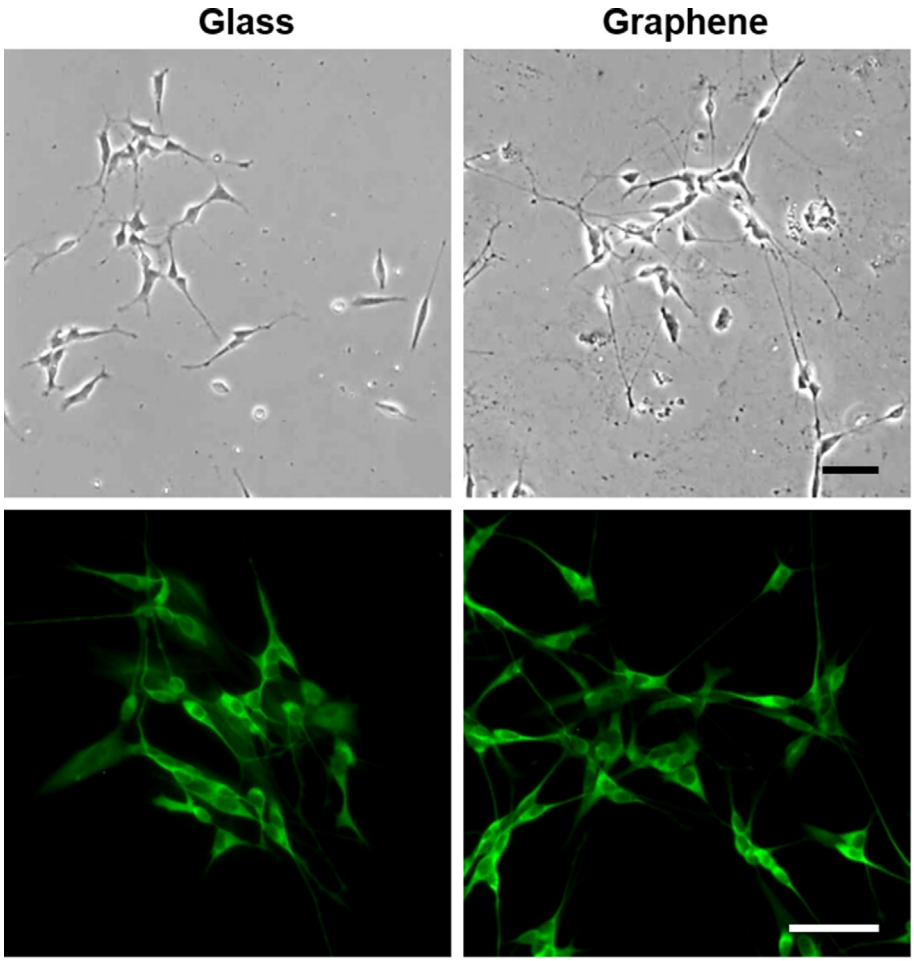

Fig. 2. Neurogenesis of SH-SY5Y human neuroblastoma cells is enhanced on graphene culture. Cells were cultured for 7 days on graphene film and glass control in the presence of RA, and optical image and immunofluorescent image of MAP2 neuronal marker were taken. Scale bar is 50 μm.

achieved through FAK or p38 MAPK. Under the ERK inhibitor, PD98059, neurite number was decreased but neurite length was not affected.

4. Discussion

In this study, a single layered graphene film could be successfully formed on a square glass slide and the neurogenesis of human neuroblastoma cells was tested with the glass slide used as a control. SH-SY5Y cells on graphene displayed significantly greater neurogenesis relative to glass control, as assessed by increased neurite length and number and upregulated expression in key neuronal genes. Importantly, such stimulations were achieved even in the absence of soluble neurogenic factor, RA. Inhibitor studies suggested that focal adhesion signaling (FAK) or mitogen-activated protein kinase signaling (p38) may be involved in the graphene induction of cellular neurogenesis.

A few reported data suggest that graphene has a potential to positively regulate the behavior of several cells including MSCs, neuronal cells, and endothelial cells [8–12]. However, it is still premature to conclude on the cytocompatibility of graphene. Importantly, graphene substrates utilized in these previous reports have limitations for systematic cytocompatibility tests. For example, graphene films were not uniformly fabricated on glass substrate, e.g., single or multiple layers depending on the position [9]. In some studies, multiple layers of graphene sheets were formed on the portion of the TCPS dish and neuronal cell behavior was studied by culturing cells on this part graphene/part TCPS substrate [10,11]. This approach may be allowed for imaging of the cells but not be applicable for gene/protein expression assays that require cell lysates from each part of the substrate, graphene and TCPS. Furthermore, one cannot exclude the possibility that cells grown in each part may interact each other by secreting and communicating soluble signals. In our study, a monolayer graphene film could be successfully produced on the glass coverslip with no uncoated portion (Fig. 1, optical images and Raman/UV–vis–NIR spectra indicating monolayer formation). Via these substrates, cell behaviors, both imaging and gene expression data, could be examined in a well-controlled systematic manner with appropriate controls.

Graphene induced significantly greater neurite outgrowth relative to the glass control (Figs. 2 and 3). Interestingly, cells cultured on graphene even without the stimulation by RA soluble signal could trigger neurite processes, producing significantly longer and more neurites relative to the glass no RA control (Fig. 3B). The neurite outburst number on the graphene culture without RA was comparable to that of the RA treatment alone case on glass. Further, specific neuronal gene expression, NFL, showed a remarkable upregulation with pure graphene culture even in the absence of RA (Fig. 3C). As a note, in our recent study on the mechanical control of cellular neurogenesis, NFL expression was responsive to the mechanical cell stretch stimulation [16].

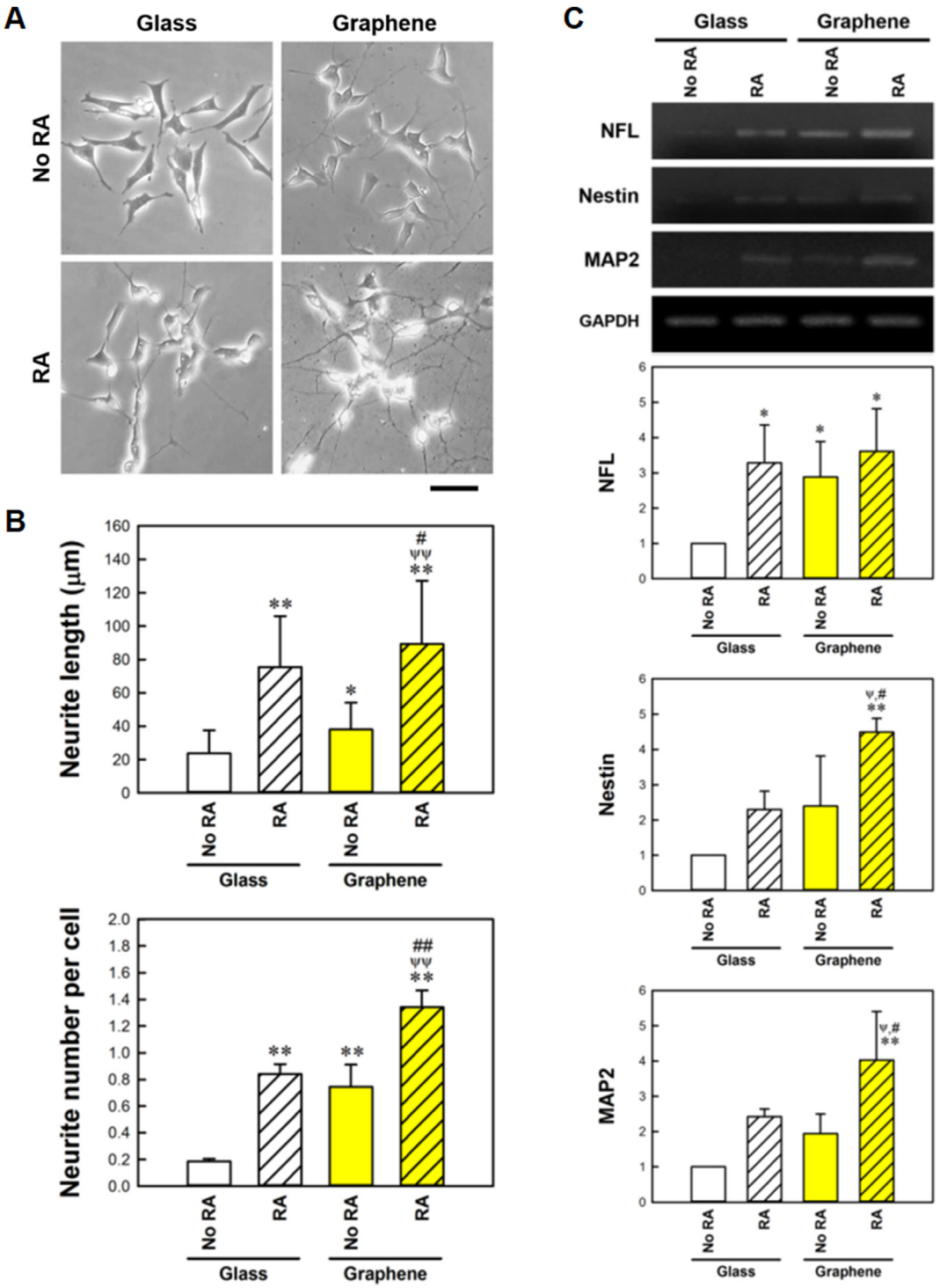

Fig. 3. Neurite length and number per cell and neuronal gene expression are increased for cells on graphene. (A) Cells were cultured for 7 days on glass and graphene without or with RA. Scale bar is 50 μm. (B) RA induced longer and more neurites on both glass and graphene substrates. Graphene culture alone could induce neurite outgrowth, and this effect was further increased with RA exposure. Means and standard deviations are presented. (C) NFL expression was increased by graphene even in the absence of RA. Nestin and MAP2 could be detected on graphene without RA, relative to no detection on the glass no RA control. Means and standard deviations are presented. *: $p < 0.05$ and **: $p < 0.01$ compared with glass no RA control. $^{\psi}$: $p < 0.05$ and $^{\psi\psi}$: $p < 0.01$ compared with graphene no RA control. $^{\#}$: $p < 0.05$ and $^{\#\#}$: $p < 0.01$ for comparisons between glass and graphene under RA.

Combined data may suggest the role of NFL, a key intermediate filament in neurons and axons, as a governing molecular senor responsive to substrate and mechanophysical extracellular cues. The other neuronal markers, nestin and MAP2, could also be detected on graphene in comparison with no detection on glass no RA control. Our observations that the stimulatory effects from pure graphene culture are comparable to those of the RA soluble cue suggest a potential of graphene to be exploited as a platform for neurogenesis-inductive substrate. Since graphene and RA showed in general synergistic effects (Fig. 3), finding an optimal RA concentration to maximize the stimulatory effect from graphene may suggest a combined condition for enhanced neurogenesis.

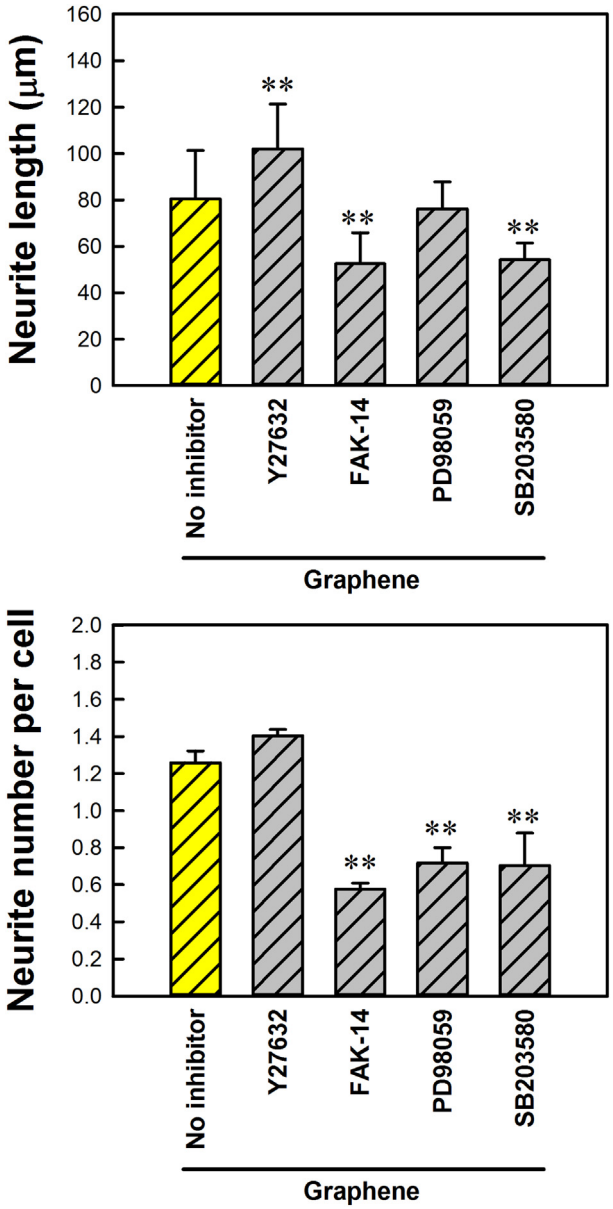

Fig. 4. FAK and p38 MAPK may mediate the graphene stimulation of cell neurogenesis. Cells were cultured on graphene for 7 days with RA and also with molecular inhibitors of ROCK (Y27632), FAK (FAK-14), ERK (PD98059), and p38 MAPK (SB203580). Inhibiting FAK and p38 decreased both neurite length and number compared with graphene no inhibitor control. Inhibiting ERK reduced neurite number per cell. ROCK inhibition increased neurite length. **: $p < 0.01$ compared with graphene no inhibitor control.

It is not clear at this stage what material characteristics allowed graphene to have increased neural cytocompatibility. We have demonstrated that surface topographic scale has a potential to affect osteoblastic and stem cells [21,22]. In the current study, two surfaces were mostly flat with no predetermined textures (Fig. 1D) and surface roughness parameters were in the same order of magnitude (less than few nm) for both surfaces. This topographic difference may not induce changes in cell behavior. Note that we previously observed that cell functions were differentially affected when z-axis topographic scale was altered at 10 nm vs. 100 nm scale [21,22]. Another surface characteristic, substrate wettability, may also affect cells. We showed that hydrophilic (low contact angle) surfaces better support cell adhesion and spreading and bone cell differentiation than hydrophobic (high contact angle) surfaces [23,24]. As graphene was more hydrophobic (Fig. 1E), increased neural cytocompatibility on graphene might not originate from the difference in hydrophilicity. When excluding topography and wettability parameters, it may be speculated that intrinsic difference in surface chemistry, hexagonally interconnected monolayer carbon for graphene vs. SiO_2 for glass substrate, could contribute to the altered neural cell behavior.

From the inhibitor studies, it was suggested that FAK or p38 MAPK may play a role in the graphene triggering of cellular neurogenesis (Fig. 4, Fig. S1). FAK links transmembrane integrin with cytoskeleton at focal adhesion sites, mediating various cell functions including adhesion, spreading, growth, differentiation, and mechanical sensitivity [21]. FAK has also been shown to stimulate neurite outgrowth and neuronal cell migration via Rack1 and Cdk5 signaling pathways and to regulate axonal growth cone formation [25–27]. Our result showing that the graphene induction of neurite outgrowth was disrupted by FAK inhibitor (Fig. 4) implies that FAK would be involved in the graphene control of neurogenesis. It has been reported that MAPK families including p38, ERK1/2, and JNK/SAPK play a role in the survival, growth, and differentiation of neuronal cells [28]. Our data also indicate the regulatory role of p38 in the graphene control of neuronal cells. Inhibiting ERK1/2 also proposed a similar trend but only for the neurite outburst per cell. Additionally, the role of ROCK inhibition to enhance neural cell elongation, protrusion, and migration [20] was confirmed in the graphene culture.

In conclusion, to test the neural cytocompatibility of graphene and to reveal relevant molecular mechanisms, we fabricated monolayer graphene on glass substrates via CVD and wet transfer technique. Human neuroblastoma cells cultured on graphene showed significantly longer and more neurites relative to cells on the glass control. Interestingly, this was observed even in the absence of RA soluble neurogenic factor. Key genes relevant to neurogenesis (e.g., NFL) were also upregulated on graphene. Inhibitor studies suggested that the graphene induction of cellular neurogenesis may be mediated by FAK and p38 MAPK cascades. Our data suggest that graphene may be explored as a platform for neural regenerative medicine.

Conflict of interest

None.

Acknowledgments

The authors thank the funding supports from NSF CAREER Award 1351570, AHA Scientist Development Grant 12SDG12030109, Osteology Foundation grant 12-006 (all for Lim), Nebraska Research Initiative (Lim and Sinitskii), and NSF EPSCoR grant 1004094 (Sinitskii). The contact angle measurement was performed at the Center for Nanohybrid Functional Materials core facility at the University of Nebraska–Lincoln supported by National Science Foundation (EPS-1004094).

Appendix A. Supplementary data

Supplementary data related to this article can be found at http://dx.doi.org/10.1016/j.bbrc.2015.03.023.

Transparency document

Transparency document related to this article can be found online at http://dx.doi.org/10.1016/j.bbrc.2015.03.023.

References

[1] K.S. Novoselov, V.I. Fal'ko, L. Colombo, P.R. Gellert, M.G. Schwab, K. Kim, A roadmap for graphene, Nature 490 (2012) 192–200.
[2] S. Shi, F. Chen, E.B. Ehlerding, W. Cai, Surface engineering of graphene-based nanomaterials for biomedical applications, Bioconjugate Chem. 25 (2014) 1609–1619.
[3] H. Zhang, G. Grüner, Y. Zhao, Recent advancements of graphene in biomedicine, J. Mater. Chem. B 1 (2013) 2542–2567.
[4] L. Feng, L. Wu, X. Qu, New horizons for diagnostics and therapeutic applications of graphene and graphene oxide, Adv. Mater. 25 (2013) 168–186.
[5] X. Huang, Z. Zeng, Z. Fan, J. Liu, H. Zhang, Graphene-based electrodes, Adv. Mater. 24 (2012) 5979–6004.
[6] H. Shen, L. Zhang, M. Liu, Z. Zhang, Biomedical applications of graphene, Theranostics 2 (2012) 283–294.
[7] M. Perán, M.A. García, E. López-Ruiz, M. Bustamante, G. Jiménez, R. Madeddu, J.A. Marchal, Review: functionalized nanostructures with application in regenerative medicine, Int. J. Mol. Sci. 13 (2012) 3847–3886.
[8] T.R. Nayak, H. Andersen, V.S. Makam, C. Khaw, S. Bae, X. Xu, P.L. Ee, J.H. Ahn, B.H. Hong, G. Pastorin, B. Özyilmaz, Graphene for controlled and accelerated osteogenic differentiation of human mesenchymal stem cells, ACS Nano 5 (2011) 4670–4678.
[9] G.Y. Chen, D.W. Pang, S.M. Hwang, H.Y. Tuan, Y.C. Hu, A graphene-based platform for induced pluripotent stem cells culture and differentiation, Biomaterials 33 (2012) 418–427.
[10] N. Li, X. Zhang, Q. Song, R. Su, Q. Zhang, T. Kong, L. Liu, G. Jin, M. Tang, G. Cheng, The promotion of neurite sprouting and outgrowth of mouse hippocampal cells in culture by graphene substrates, Biomaterials 32 (2011) 9374–9382.
[11] M. Tang, Q. Song, N. Li, Z. Jiang, R. Huang, G. Cheng, Enhancement of electrical signaling in neural networks on graphene films, Biomaterials 34 (2013) 6402–6411.
[12] M. Guo, M. Li, X. Liu, M. Zhao, D. Li, D. Geng, X. Sun, H. Gu, N-containing functional groups induced superior cytocompatible and hemocompatible graphene by NH_2 ion implantation, J. Mater. Sci. Mater. Med. 24 (2013) 2741–2748.
[13] X. Li, W. Cai, J. An, S. Kim, J. Nah, D. Yang, R. Piner, A. Velamakanni, I. Jung, E. Tutuc, S.K. Banerjee, L. Colombo, R.S. Ruoff, Large-area synthesis of high-quality and uniform graphene films on copper foils, Science 324 (2009) 1312–1314.
[14] A. Lipatov, A. Varezhnikov, M. Augustin, M. Bruns, M. Sommer, V. Sysoev, A. Kolmakov, A. Sinitskii, Intrinsic device-to-device variation in graphene field-effect transistors on a Si/SiO_2 substrate as a platform for discriminative gas sensing, Appl. Phys. Lett. 104 (2014) 013114.
[15] I. Poudel, J.S. Lee, L. Tan, J.Y. Lim, Micropatterning-retinoic acid co-control of neuronal cell morphology and neurite outgrowth, Acta Biomater. 9 (2013) 4592–4598.
[16] S. Higgins, J.S. Lee, L. Ha, J.Y. Lim, Inducing neurite outgrowth by mechanical cell stretch, BioRes. Open Access 2 (2013) 212–216.
[17] A.C. Ferrari, J.C. Meyer, V. Scardaci, C. Casiraghi, M. Lazzeri, F. Mauri, S. Piscanec, D. Jiang, K.S. Novoselov, S. Roth, A.K. Geim, Raman spectrum of graphene and graphene layers, Phys. Rev. Lett. 97 (2006) 187401.
[18] R.R. Nair, P. Blake, A.N. Grigorenko, K.S. Novoselov, T.J. Booth, T. Stauber, N.M. Peres, A.K. Geim, Fine structure constant defines visual transparency of graphene, Science 320 (2008) 1308.
[19] T. Frappier, F. Stetzkowski-Marden, L.A. Pradel, Interaction domains of neurofilament light chain and brain spectrin, Biochem.. J. 275 (1991) 521–527.
[20] K.J. Christie, A. Turbic, A.M. Turnley, Adult hippocampal neurogenesis, Rho kinase inhibition and enhancement of neuronal survival, Neuroscience 247 (2013) 75–83.
[21] J.Y. Lim, A.D. Dreiss, Z. Zhou, J.C. Hansen, C.A. Siedlecki, R.W. Hengstebeck, J. Cheng, N. Winograd, H.J. Donahue, The regulation of integrin-mediated osteoblast focal adhesion and focal adhesion kinase expression by nanoscale topography, Biomaterials 28 (2007) 1787–1797.
[22] J.Y. Lim, A.E. Loiselle, J.S. Lee, Y. Zhang, J.D. Salvi, H.J. Donahue, Optimizing the osteogenic potential of adult stem cells for skeletal regeneration, J. Orthop. Res. 29 (2011) 1627–1633.
[23] X. Liu, J.Y. Lim, H.J. Donahue, R. Dhurjati, A.M. Mastro, E.A. Vogler, Influence of substratum surface chemistry/energy and topography on the human fetal osteoblastic cell line hFOB 1.19: phenotypic and genotypic responses observed in vitro, Biomaterials 28 (2007) 4535–4550.
[24] J.Y. Lim, M.C. Shaughnessy, Z. Zhou, H. Noh, E.A. Vogler, H.J. Donahue, Surface energy effects on osteoblast spatial growth and mineralization, Biomaterials 29 (2008) 1776–1784.
[25] S. Dwane, E. Durack, R. O'Connor, P.A. Kiely, RACK1 promotes neurite outgrowth by scaffolding AGAP2 to FAK, Cell. Signal 26 (2014) 9–18.
[26] Z. Xie, L.H. Tsai, Cdk5 phosphorylation of FAK regulates centrosome-associated miocrotubules and neuronal migration, Cell Cycle 3 (2004) 108–110.
[27] M.R. Chacón, P. Fazzari, FAK: dynamic integration of guidance signals at the growth cone, Cell. Adh. Migr. 5 (2011) 52–55.
[28] M. Miloso, A. Scuteri, D. Foudah, G. Tredici, MAPKs as mediators of cell fate determination: an approach to neurodegenerative diseases, Curr. Med. Chem. 15 (2008) 538–548.